Carbohydrate Research 344 (2009) 1709–1715

Contents lists available at ScienceDirect

Carbohydrate Research

journal homepage: www.elsevier.com/locate/carres

Chitosan membranes modified by contact with poly(acrylic acid)

M. S. P. De Lima, M. S. Freire, J. L. C. Fonseca, M. R. Pereira *

Departamento de Química, Universidade Federal do Rio Grande do Norte, Lagoa Nova, Natal, CP1662, RN 59078-970, Brazil

ARTICLE INFO

Article history:
Received 23 January 2009
Received in revised form 12 May 2009
Accepted 28 May 2009
Available online 2 June 2009

Keywords:
Chitosan membrane
Poly(acrylic acid)
Permeability
Polyelectrolyte complex

ABSTRACT

In this work chitosan membranes modified by contact with poly(acrylic acid) (PAA) aqueous solution at two different temperatures (25 °C and 60 °C) were obtained. The pure chitosan (CS) membranes, as well as those treated with PAA (CSPAA_25 and CSPAA_60) were characterized by FTIR-ATR, water sorption capacity, thermal analysis (TG/DTG), and scanning electron microscopy (SEM). In addition, in vitro permeation experiments were carried out using metronidazol and sodium sulfamerazine aqueous solutions at 0.1% and 0.2% as model drugs. FTIR-ATR results showed the presence of absorption bands of NH_3^+ and COO^- indicating the formation of a polyelectrolyte complex between chitosan and poly(acrylic acid). The results also indicated that PAA penetrates deeper into the membrane at higher temperature (60 °C), forming a thicker complex layer. Polyelectrolyte complex formation as well as the influence of treatment temperature was confirmed by lower hydrophilicity, higher thermal stability, and lower permeability of the treated membranes. The results show that the methodology used is a simple and very efficient way to drastically change some membrane properties, especially their permeability.

1. Introduction

The technology associated to the modification of pharmaceutical formulations for drug release has progressed significantly in the last decade. Nowadays, in addition to the traditional formulations, five new forms stand out: tablets coated with semi permeable membranes,[1] transdermic adhesives,[2] subcutaneous implants,[3] microspheres,[4] and liposomes.[5] In all these formulations, a biomaterial must always be used in order to control drug release. Among the biomaterials, biodegradable hydrogels have emerged as an important class, not only owing to their biocompatibility but also because their degradation products are not immunogenic, carcinogenic, or toxic to human beings.[6] The drug release rate in such systems can be controlled by polymeric properties such as swelling capacity, degradability, porosity, and permeability. Several natural and synthetic polymers have been investigated, for example, poly(acrylic acid),[7] hyaluronic acid,[8] collagen,[9] and chitosan.[4] Chitosan is a natural, biodegradable, and biocompatible polymer, derived from the partial deacetylation reaction of chitin, one of the most abundant linear chain polysaccharides occurring as a major fraction of insects and crustaceans exoskeleton. Chitosan can be defined as a copolymer of 2-amino-2-deoxy-D-glucopyranose and 2-acetoamido-2-deoxy-D-glucopyranose whose units are linked by β(1→4) bonds. In acidic medium, chitosan is a cationic polyelectrolyte due to the protonation of its NH_2 groups.[10] As a polycation, chitosan can form electrostatic complexes with negatively charged species including proteins, anionic polymers, and drugs. These polymeric complexes are formed by the association of two polymers through electrostatic attractions, hydrogen bonds, van de Walls interactions, or a combination of these.[11–13] Such complex formation is directly dependent on the ionization degree of both polymers (pH and ionic strength), charge density (chain conformation), and concentration.[11] Polyelectrolyte complexes (PEC) can be used in the form of hydrogels, films, and membranes. The literature describes several studies on polyelectrolyte complexes suitable for biomedical applications as, those composed of chitosan and sulfonated polystyrene,[14] poly(acrylic acid) (PAA),[15] alginate,[16] and pectin.[17] The chitosan and PAA complexes are formed to reduce PAA solubility in water. Studies have shown that PAA solubility can be reduced, while its mucoadhesive properties can be improved or maintained.[18] The insolubility is generated by the strong electrostatic interactions that occur between the ammonium ion from chitosan and the carboxylate ion, from PAA, inducing a physical crosslinking and therefore, preventing dissolution and excessive swelling of the polymeric matrix in water. According to the literature, the polyelectrolyte complexes of chitosan and PAA can be obtained by the physical mixture of both polymers, under fusion, by polymers dissolution in one solvent followed by solvent evaporation or by template polymerization.[19,20] Another possibility is to obtain these complexes by PAA diffusion from the surface of a previously prepared chitosan membrane, using different temperatures. As far as can be determined, the last technique has been insufficiently explored.[21] Therefore the aim of this study was to prepare these polyelectrolyte membranes and to study their permeability characteristics with respect to two different drugs.

* Corresponding author.
E-mail address: mrp03@uol.com.br (M.R. Pereira).

0008-6215/$ - see front matter © 2009 Elsevier Ltd. All rights reserved.
doi:10.1016/j.carres.2009.05.024

2. Materials and methods

Chitosan was obtained from Polymar Ltd (Brazil) with a degree of deacetylation of 90%, according to the supplier. Metronidazol (MM = 171.5 g/mol) (Aldrich, USA) and sodium sulfamerazine (MM = 286 g/mol) (Aldrich, USA) were both R&D grade. Poly(-acrylic acid) Mw = 250,000 Da) (Aldrich, USA) and all the other chemical reagents were of analytical grade and used as received.

2.1. Membrane preparation

2.1.1. Chitosan membranes

Chitosan was dissolved in a 2.0% v/v aqueous acetic acid solution for 24 h under mechanical stirring in order to form a 1.5% w/v solution. The resulting solution was filtered using a Millipore® Millex filter, with 40 μm of pore diameter. The solution was then left to stand for 2 h to allow bubbles evolution. A solution volume of 25 ml was cast onto a glass plate and left in an oven at 50 °C for 24 h for solvent evaporation. The membranes were then immersed in a 5.0% sodium hydroxide (NaOH) solution for 2 h, to be neutralized. Afterwards, they were repeatedly washed with distilled water and allowed to dry at room temperature. These membranes were denominated CS membranes.

2.1.2. Treatment with poly(acrylic acid)

Chitosan/poly(acrylic acid) membranes were prepared from pure chitosan membranes obtained as described above. The chitosan membranes were fixed on a support. A volume of 50 ml of 2.0 g/L aqueous solution of poly(acrylic acid) was placed in contact with the upper side of the chitosan membrane for 2 h. The experiments were done at room temperature and at 60 °C. The membranes were then removed from the support, washed with distilled water, and dried at room temperature. These membranes were denominated CSPAA_25 and CSPAA_60 for room temperature and 60 °C, respectively. Membranes' thicknesses were measured using a digital micrometer Check line model DCF 900. The values considered for permeability calculation purpose represent an average of ten measurements done at different points and sides of a membrane.

2.2. Membrane characterization

2.2.1. FTIR-ATR

The infrared spectra were obtained using a Thermo Nicolet Nexus 470 FTIR spectrometer. The membranes were analyzed using a variable angle attenuated total reflection (ATR) accessory, with a ZnSe crystal using incidence angles of 39°, 45°, and 60°. The spectra were obtained for both sides of the membranes. The sample names contain the incident angle used, the side of the membrane (CSPAA for the treated side and CS for the non-treated side), and the temperature used, for example, 39_CSPAA_25, and 39_CS_25 for the treated and non-treated side, respectively.

2.2.2. Water sorption capacity

The water sorption capacity of membranes was estimated using a mass balance (B-TEC-U210A, TECNAL, Brazil) at room temperature. The dry membranes were weighted and then immersed in distilled water. At time intervals of 0.25, 0.5, 1, 2, 3, 4, 5, 6, 24, and 48 h the membranes were removed from the water, wiped off, weighted, and returned to the water. The water sorption capacity, $W(\%)$ was calculated according to Eq. 1:

$$W(\%) = \left(\frac{m_w - m_d}{m_d}\right)100 \quad (1)$$

where m_w and m_d are the mass of wet and dry membrane, respectively. In these experiments, 5 samples were analyzed for each type of membrane.

2.2.3. Thermogravimetric analysis (TGA)

A Shimadzu DTG-60 thermogravimetric analyzer was used to study the thermal stability of the membranes. Samples of 5 mg were submitted to a heating rate of 10 °C/min in nitrogen atmosphere and at a temperature range between 25 °C and 800 °C.

2.2.4. Scanning electron microscopy (SEM)

Fragments consisting of 0.25 cm^2 squares were cut from the center of the membranes, placed on a proper aluminum support and sputter coated with a thin gold layer. The images were obtained by a Philips XL30 SEM (Netherland) using a tungsten filament, secondary electrons detector, and a voltage of 20 kV.

2.3. Permeability tests

The permeability coefficients of two model drugs were determined using a two compartmented cell with 230 ml of capacity each, described elsewhere.[15,22,23] The membrane area was 8.46 cm^2. The solutions, inside the compartments, were mechanically stirred. Sodium sulfamerazine and metronidazol were chosen for the experiments. Before the test, the membranes were swollen in water for 12 h until a state of equilibrium was reached. The right side of the cell was filled with drug solution at concentrations of 0.1% and 0.2% for both drugs. The left side of the cell was always filled with distilled water. During the experiment the right side concentration was considered constant. A continuous flux system was attached to the left side of the cell in order to determine the solution absorbance at λ = 260 nm for sodium sulfamerazine and λ = 320 nm for metronidazol using a UV–vis Spectrometer (Varian Cary 100). The temperature was kept constant at 30.0 °C ± 0.1 °C, by means of a thermostatic bath. All the experiments were run in duplicate.

The permeability coefficient (P), was calculated using the model described by Crank[24] for flux through a membrane, adapted to measurements of absorbance:[23]

$$P = \frac{\alpha V l}{C_1 \varepsilon b S} \quad (2)$$

where α is the angular coefficient of the curve generated by the plot of absorbance versus time, V is the cell volume, l membrane thickness, C_1 initial drug concentration, ε absorptivity, b the UV–vis cell pathway, and S the membrane area.

3. Results and discussion

3.1. Infrared spectroscopy

The FTIR-ATR technique with variable angle was used to obtain more surface representative spectra. To determine the range of the angles to be used, the critical angle θ_c was determined by Eq. (3):[25]

$$\theta_c = \sin^{-1}\left(\frac{n_1}{n_2}\right) \quad (3)$$

where n_1 is the refractive index for the ZnS crystal (n_1 = 2.40)[26] and n_2 for chitosan (n_2 = 1.50).[27] Since the calculated critical angle was 38.9°, the chosen incident angles were 39°, 45°, and 60°. Table 1 shows a number of characteristics for each incident angle used.[28] From Table 1 it can be observed that, as the incidence angle increases, the number of reflections and depth of penetration decrease. Therefore, by using an incidence angle of 60° it is possible to obtain a more surface representative spectrum than that

Table 1
Parameters related to the incident angles used

θ_{scale} (°)	$\theta_{effective}$ (°)	Number of reflections	d_p (μm) for $\bar{\nu}$ = 1600 cm^{-1}
39	41.2	19.0	5.32
45	45.0	16.6	1.25
60	54.0	12.1	0.69

d_p—penetration depth.

obtained at 39°. All spectra were obtained using the hydrated membranes and their thicknesses were 70 ± 5 μm.

Figure 1 shows the spectra for both sides of one membrane treated with PAA at room temperature, using incidence angles of 39° (a), 45° (b), and 60° (c). According to the literature,[29,30] the wavenumber range corresponds to the region where the complex formation between chitosan and PAA can be observed. The remaining regions of the spectrum showed no variations for the three incident angles used. Figure 2 shows that the spectrum obtained at 45° and especially the one obtained at 60° exhibits a new band, near 1560 cm^{-1} which, according to the literature, corresponds to the absorption characteristics of NH_3^+ and COO^- groups, indicating a complex formation. The spectra at 39° showed no significant differences between two sides of the membrane.

The differences that occurred as a function of the incidence angle used can be explained by the difference in the penetration depth (d_p) of the evanescent field shown in Table 1. As the table demonstrates, the incidence angle of 60° had the lowest d_p value

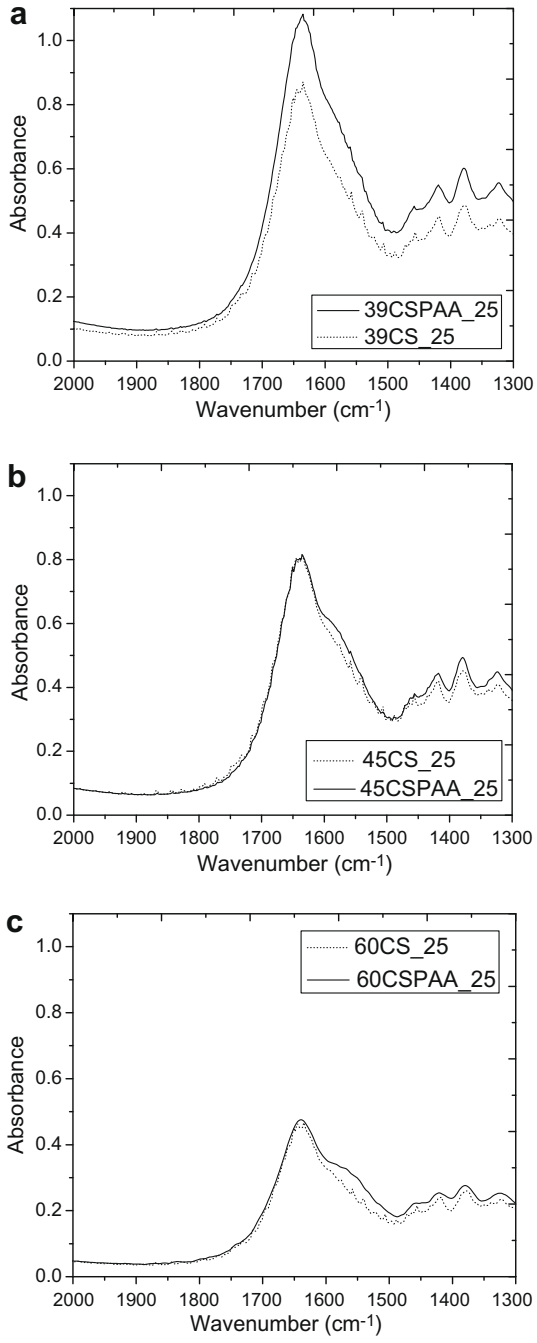

Figure 1. FTIR-ATR spectra for both sides of chitosan membrane surface treated with poly(acrylic acid), at room temperature for incident angles of 39° (a), 45° (b), and 60°(c).

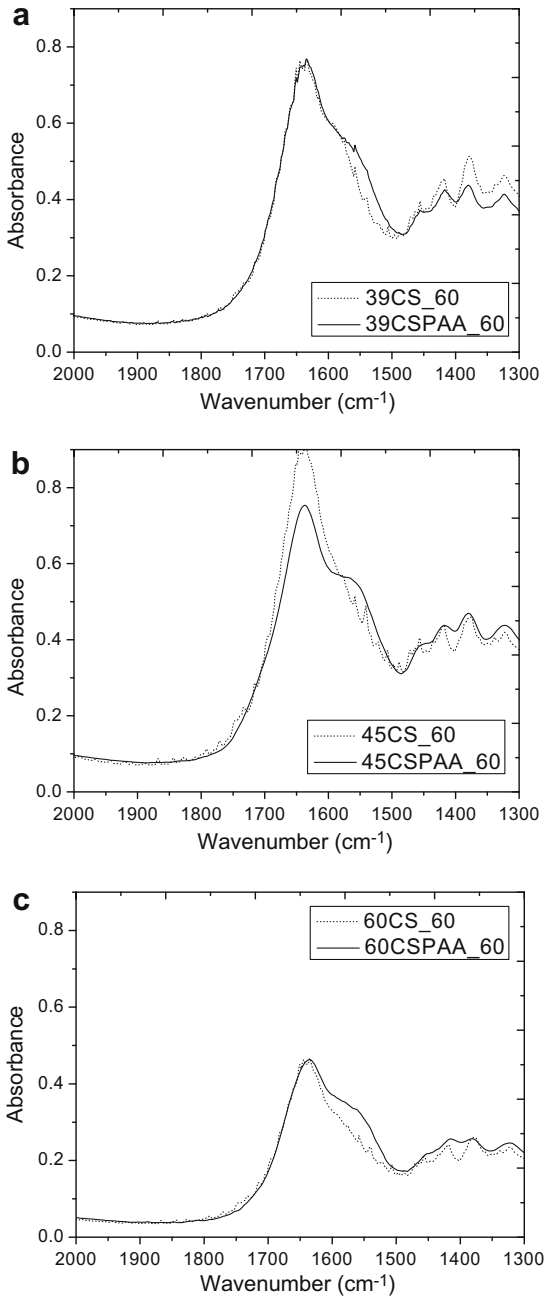

Figure 2. FTIR-ATR spectra for both sides of chitosan membrane surface treated with poly(acrylic acid), at 60 °C for incident angles of 39° (a), 45° (b), and 60°(c).

and therefore, is the most representative of the sample surface. On the other hand, the spectrum obtained at 39° had a 7-time greater penetration depth, obtaining information not only from the surface but also from the bulk. These results confirm that the PAA treatment was superficial, with a penetration of few micra and, as a consequence, the membranes obtained were asymmetric. Figure 2 shows the same spectra sequence as Figure 1 but using membranes treated with PAA at 60 °C. In this case it can be observed that even at 39°, the emergence of a new band, characteristic of the complex formation, can be seen and that as the incident angle increases this absorption becomes more intense. These results indicate that an increase in temperature allows PAA to penetrate more deeply inside the membranes making the complex layer thicker, and observed even at 39°. A possible explanation is the fact that at 60 °C, chitosan is probably above its glass transition temperature,[31] in a rubbery state where the chains have higher mobility, facilitating the penetration of PAA molecules.

3.2. Water sorption capacity

Figure 3 shows the results of water sorption capacity for the three membranes under investigation. All membranes exhibited water sorption values above 100%, an indication of the strong water affinity of both, chitosan and PAA. In the case of chitosan it is known that this hydrophilicity is due to the presence of amino and hydroxyl groups in its structure whereas, in the case of PAA, it is due to the presence of carboxylic groups that confer, water solubility on this material. The results also show that with PAA treatment, the membranes had decreased water sorption capacity and that, the higher the treatment temperature, the lower the membrane hydrophilicity. The results confirm the complex formation since even with the addition of a water soluble polymer, membrane water sorption is reduced. This occurred because the interaction between the NH_3^+ and COO^- groups induces physical crosslinking on the membrane surface layer and, as a consequence, decreases its water sorption capacity.[15]

3.3. Thermal analysis (TG, DTG)

Figure 4 shows the DTG curves for CS, CSPAA_25, and CSPAA_60. The chitosan thermogram shows a typical polysaccharide behavior, exhibiting two distinct stages of degradation. The first one starts at 30 °C and continues up to 200 °C with a maximum at 52.6 °C and a weight loss of 10.3%. The second stage starts at about 200 °C and extends to 400 °C with a maximum peak around 300 °C and weight loss of 49.5%. CSPAA_25 and CSPAA_60 DTG curves also displayed two stages of degradation. CSPAA_25 membrane has a first stage with a maximum at 58.9 °C and weight loss of 7.7% and a second stage with a maximum at 300 °C and weight loss of 35.0%. CSPAA_60 has a maximum peak at 59.2 °C and weight loss of 6.8% for the first stage and a maximum at 300 °C with weight loss of 34.6% for the second stage.

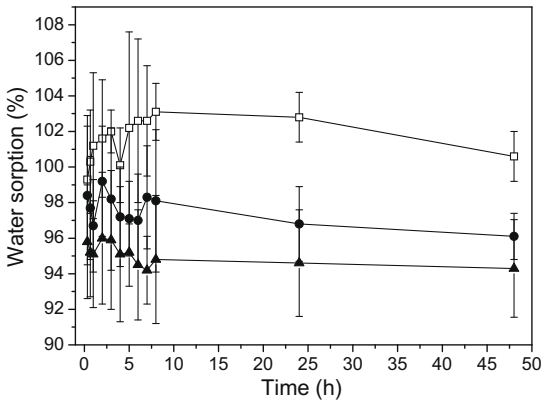

Figure 3. Water sorption capacity for pure chitosan (open square), CSPAA_25 (full circle), and CSPAA_60 membranes (full triangle).

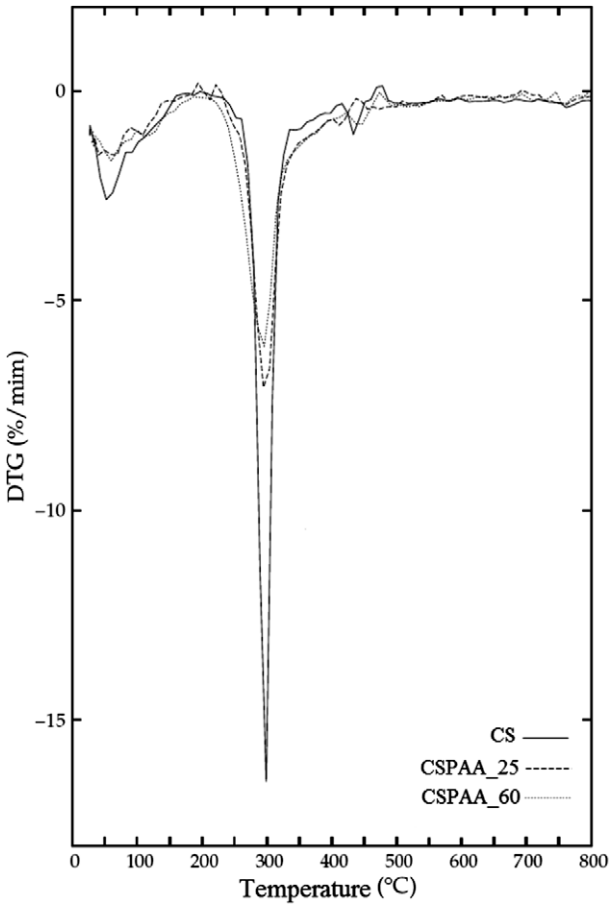

Figure 4. Differential thermo gravimetric analysis for pure chitosan, CSPAA_25, and CSPAA_60 membranes.

According to the literature,[31,32] the first stage for chitosan is related to the loss of water molecules associated by hydrogen bonds, to the amino and hydroxyl groups of this polymer. Changes in this stage are related not only to the amount of water absorbed by the membrane but also to the strength of water-chitosan interactions. Comparing the thermograms for pure and treated membranes, it can be observed that the water release temperature is similar for the three membranes, indicating that chitosan–water interactions are analogous. However, there was a decrease in weight loss for CSPAA_25 and another, even more accentuated, for CSPAA_60. These results confirm the effect of the PAA treatment, given that some of the amino groups that acted as sites for water sorption were now forming polyelectrolyte complexes with poly(acrylic acid) and, as a consequence, the treated membranes had their water sorption capacity reduced. It has also been observed that the reduction is even higher for CSPAA_60, confirming that in such a membrane the complex formation process occurred to a greater extension, as already shown using the FTIR-ATR technique.

The second stage of degradation for chitosan is assigned to a complex process of degradation that starts with the random break of glycoside bonds followed by decomposition of acetylated and deacetylated units of the polymer. In such stage it can be observed (Fig. 6) that the weight loss follows the order CS > CSPAA_25 > CSPAA_60 indicating that the complex formation acts as a physical

crosslinking increasing, as a consequence, the membrane thermal stability.

3.4. Scanning electron microscopy

SEM of CS membrane surfaces, treated with PAA at room temperature and 60 °C, is shown in Figure 5. For CS membranes (data not shown) the SEM results showed that there are no significant differences between the side that dries in contact with the air and the other side that is in contact with the Petri dish. They are both homogeneous and the presence of porosity was not observed. For the treated membranes, the results are quite different. Figure 5 shows that the surface treated with PAA at room temperature exhibited a more wrinkled pattern than the untreated surface, whereas the one treated at 60 °C the wrinkled pattern becomes even more evident. These results can be better observed in Figure 6 that presents a higher magnification. The results confirm that PAA does not penetrate completely through the chitosan membrane, but rather is concentrated in a surface layer, whose thickness depends on the treatment temperature. This behavior is probably due to the high molecular weight of the PAA used, resulting in low mobility and impeding its diffusion through the CS membrane. As a consequence the membranes obtained were asymmetric, that is, they had a layer composed of CS-PAA polyelectrolyte complex and the bulk of pure chitosan.

3.5. Permeability tests

A series of experimental results for permeation of metronidazol (Fig. 7a) and sodium sulfamerazine (Fig. 7b) at different concentrations, using CS, CSPAA_25, and CSPAA_60 membranes are shown for illustrative purposes. It can be seen that the absorbance versus time plots yield straight lines and display good reproducibility. The slope of these lines can be used to calculate the permeability coefficient (*P*), as indicated in Eq. 2. The calculated values of *P* for different membranes, (CS, CSPAA_25, and CSPAA_60), and drug concentrations (0.1%, and 0.2%) are summarized in Table 2. The analysis from pure chitosan shows that permeability values were not affected by drug concentration, at least for the concentration range analyzed in this work. Similar results were also obtained by studying the permeability of isoniazide and amytriptiline.[22] Such independence between concentration and permeability might indicate that, at this concentration range, the membrane has already reached its saturation. The results of the surface-treated membranes show a quite different situation. First the permeability values decrease for CSPAA_25 and even more so for CSPAA_60 compared with those for pure chitosan. Second, there is a tendency toward decrease in permeability with an increase in concentration. The decrease in the permeability values of treated membranes may be a consequence of the complex formations between chitosan and PAA that, would reduce membrane perme-

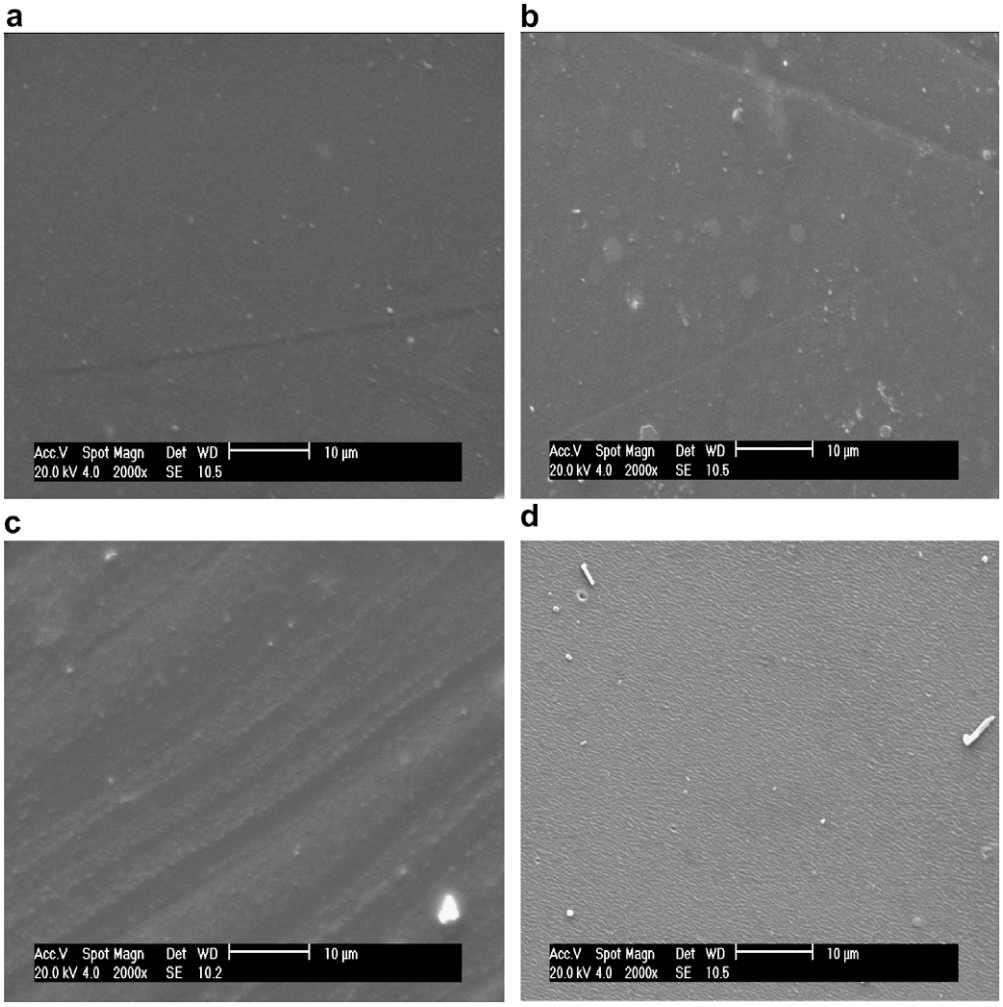

Figure 5. Scanning electron microscopy for (a) CSPAA_25 membranes non-treated, (b) CSPAA_60 non-treated, (c) CSPAA_25 treated with PAA at room temperature, and (d) CSPAA_60 treated with PAA at 60 °C.

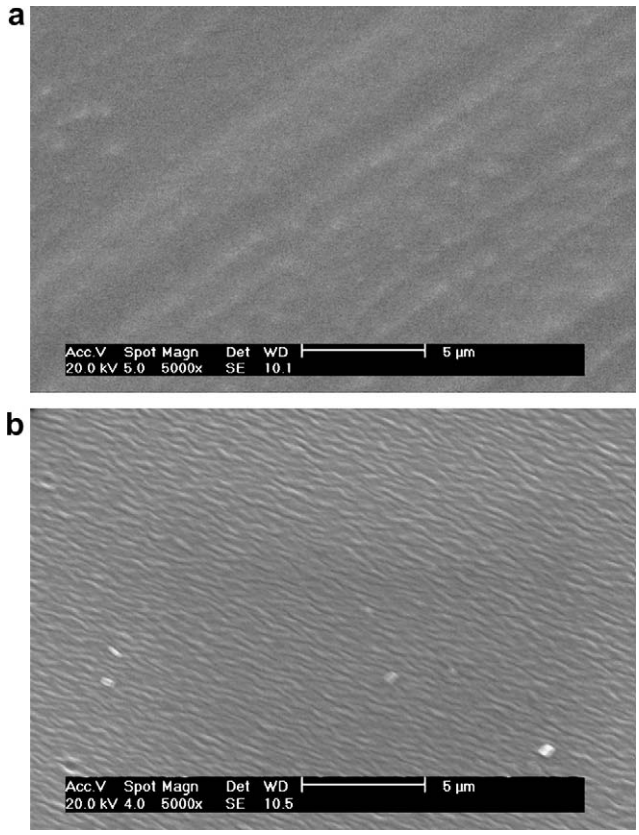

Figure 6. Scanning electron microscopy for treated surface of (a) CSPAA_25 and (b) CSPAA_60 membranes.

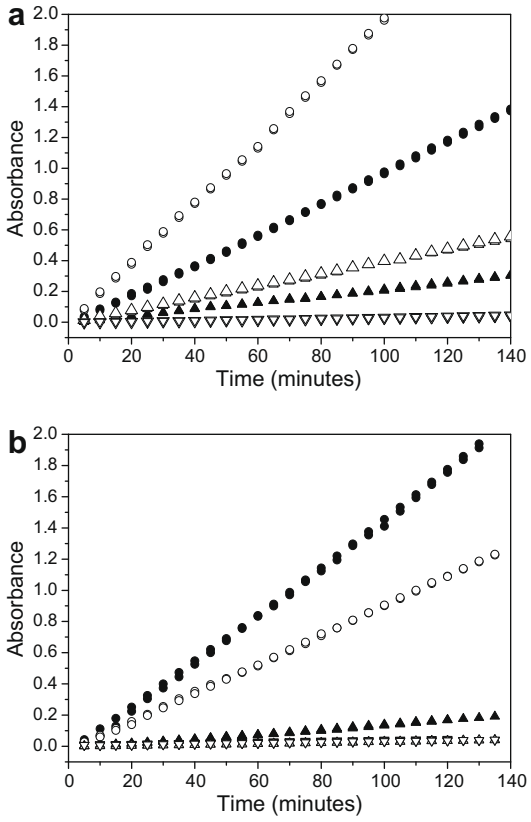

Figure 7. (a) Absorbance versus time curves for CS (circles), CSPAA_25 (up triangles), and CSPAA_60 (down triangles) using metronidazol at 0.1% (full symbols)) and 0.2% (open symbols) and (b). Absorbance versus time curves for CS (circles), CSPAA_25 (up triangles), and CSPAA_60 (down triangles) using sulfamerazine at 0.1% (full symbols)) and 0.2% (open symbols).

ability, by physically crosslinking a surface layer. The results also confirm that at 60 °C PAA macromolecules are able to penetrate deeper inside the membrane, creating a thicker layer of crosslinked material that would act as a barrier to the permeation of the analyzed drugs. Table 2 shows that permeability values for sodium sulfamerazine are lower than for metronidazol for all analyzed membranes. This behavior is probably related to the molecular dimensions of the drugs, which are directly related to their molecular weight (171 g/mol for metronidazol and 286 g/mol for sodium sulfamerazine). This difference in permeability shows that chitosan membranes and especially the one superficially treated with PAA can be quite specific in terms of these two drugs, and more selective with respect to sodium sulfamerazine.

Table 2
Permeability coefficients for CS, CSPAA_25, and CSPAA_60 membranes using sodium sulfamerazine (SMZ), and metronidazol (MDZ) at different concentrations

	Permeability coefficient ($P \times 10^6$) (cm^2/s)		
	CS	CSPAA_25	CSPAA_60
MTZ0.1%	35 ± 1.2	7.0 ± 0.1	1.00 ± 0.02
MTZ0.2%	34 ± 1.5	6.5 ± 0.1	0.60 ± 0.02
SMZ0.1%	25 ± 0.2	1.09 ± 0.02	0.81 ± 0.09
SMZ0.2%	25 ± 0.3	2.78 ± 0.05	0.38 ± 0.04

4. Conclusions

The results discussed above allow us to conclude that the diffusion process of PAA molecules through the chitosan membranes led to the formation of a polyelectrolyte complex between chitosan and PAA identified by the appearance of a new absorption band at 1560 cm^{-1}. Through FTIR-ATR we were also able to conclude that temperature is a key factor in controlling the thickness of the complex layer. The surface morphology of the membranes was altered only on the treated side, generating asymmetric membranes. The surface treatment with PAA and consequently the polyelectrolyte complex formation reduced the membranes' water sorption capacity, increased their thermal stability, and drastically reduced their permeability with respect to sodium sulfamerazine and metronidazol. The methodology used proved to be a simple and very efficient way of drastically changing some membranes' properties, especially those related to their permeability capacity.

Acknowledgment

The authors would like to thank the Brazilian agency CNPq for financial support of this work.

References

1. Zhang, Y.; Zhang, Z. R.; Wu, F. *J. Controlled Release* **2003**, *89*, 47–55.
2. Wokovich, A. M.; Prodduturi, S.; Doub, W. H.; Hussain, A. S.; Buhse, L. F. *Eur. J. Pharm. Biopharm.* **2006**, *64*, 1–8.
3. Plourde, F.; Motulsky, A.; Couffin-Hoarau, A. C.; Hoarau, D.; Ong, H.; Leroux, J. C. *J. Controlled Release* **2005**, *108*, 433–441.
4. Genta, I.; Costantini, M.; Asti, A.; Conti, B.; Montanari, L. *Carbohydr. Polym.* **1998**, *36*, 81–88.
5. Ruel-Gariepy, E.; Leclair, G.; Hildgen, P.; Gupta, A.; Leroux, J. C. *J. Controlled Release* **2002**, *82*, 373–383.
6. Lin, C. C.; Metters, A. T. *Adv. Drug Delivery Rev.* **2006**, *58*, 1379–1408.
7. Serra, L.; Domenech, J.; Peppas, N. A. *Biomaterials* **2006**, *27*, 5440–5451.
8. Kafedjiiski, K.; Jetti, R. K. R.; Foger, F.; Hoyer, H.; Werle, M.; Hoffer, M.; Bernkop-Schnurch, A. *Int. J. Pharm.* **2007**, *343*, 48–58.
9. Chan, O. C. M.; So, K. F.; Chan, B. P. *J. Controlled Release* **2008**, *129*, 135–143.

10. Rinaudo, M. *Prog. Polym. Sci.* **2006**, *31*, 603–632.
11. delaTorre, P. M.; Torrado, S.; Torrado, S. *Biomaterials* **2003**, *24*, 1459–1468.
12. delaTorre, P. M.; Enobakhare, Y.; Torrado, G.; Torrado, S. *Biomaterials* **2003**, *24*, 1499–1506.
13. delaTorre, P. M.; Torrado, G.; Torrado, S. *J. Biomed. Mater. Res. B* **2005**, *72B*, 191–197.
14. Aravind, U. K.; Mathew, J.; Aravindakumar, C. T. *J. Membr. Sci.* **2007**, *299*, 146–155.
15. DeOliveira, H. C. L.; Fonseca, J. L. C.; Pereira, M. R. *J. Biomater. Sci.-Polym. E* **2008**, *19*, 143–160.
16. Maurstad, G.; Morch, Y. A.; Bausch, A. R.; Stokke, B. T. *Carbohydr. Polym.* **2008**, *71*, 672–681.
17. Marudova, M.; MacDougall, A. J.; Ring, S. G. *Carbohydr. Res.* **2004**, *339*, 1933–1939.
18. Ahn, J. S.; Choi, H. K.; Chun, M. K.; Ryu, J. M.; Jung, J. H.; Kim, Y. U.; Cho, C. S. *Biomaterials* **2002**, *23*, 1411–1416.
19. Dhanuja, G.; Smitha, B.; Sridhar, S. *Sep. Purif. Technol.* **2005**, *44*, 130–138.
20. Wang, H. F.; Li, W. J.; Lu, Y. H.; Wang, Z. L. *J. Appl. Polym. Sci.* **1997**, *65*, 1445–1450.
21. Iwatsubo, T.; Kusumocahyo, S. P.; Shinbo, T. *J. Appl. Polym. Sci.* **2002**, *86*, 265–271.
22. Rocha, A. N. L.; Dantas, T. N. C.; Fonseca, J. L. C.; Pereira, M. R. *J. Appl. Polym. Sci.* **2002**, *84*, 44–49.
23. Neto, C. G. T.; Dantas, T. N. C.; Fonseca, J. L. C.; Pereira, M. R. *Carbohydr. Res.* **2005**, *340*, 2630–2636.
24. Crank, J. *The Mathematics of Diffusion*, 2nd ed.; Clarendon: Oxford, 1975.
25. Mirabella, F. M.; Harrick, N. J. *Internal Reflection Spectroscopy: Review and Supplement*; Harrick Scientific Corporation: Ossining, NY, 1985.
26. Stuart, B.; Ando, D. J., *Modern infrared spectroscopy*. Published on behalf of ACOL (University of Greenwich), Wiley: New York, 1996.
27. Nosal, W. H.; Thompson, D. W.; Yan, L.; Sarkar, S.; Subramanian, A.; Woollam, J. A. *Colloid Surf. B* **2005**, *46*, 26–31.
28. Mirabella, F. M.; Harrick, N. J. *Internal Reflection Spectroscopy: Review and Supplement*; Harrick Scientific Corporation: Ossining, NY, 1985. p 195.
29. de Vasconcelos, C. L.; Bezerril, P. M.; dos Santos, D. E. S.; Dantas, T. N. C.; Pereira, M. R.; Fonseca, J. L. C. *Biomacromolecules* **2006**, *7*, 1245–1252.
30. de Vasconcelos, C. L.; Bezerril, P. M.; Dantas, T. N. C.; Pereira, M. R.; Fonseca, J. L. C. *Langmuir* **2007**, *23*, 7687–7694.
31. Neto, C. G. T.; Giacometti, J. A.; Job, A. E.; Ferreira, F. C.; Fonseca, J. L. C.; Pereira, M. R. *Carbohydr. Polym.* **2005**, *62*, 97–103.
32. Peniche, C.; Arguelles-Monal, W.; Davidenko, N.; Sastre, R.; Gallardo, A.; San Roman, J. *Biomaterials* **1999**, *20*, 1869–1878.